

Effects of extended soaking time preceding roll bonding on the microstructure and mechanical properties of a modified AA3003 clad with AA4045

Joseph Moema^{1,2*}, Charles Siyasiya², Veronica Morudu¹, Nomsombuluko Hadebe³, Maje Phasha¹ and Thokozani Buthelezi⁴

¹Advanced Materials Division, MINTEK, Randburg, South Africa.

²Department of Material Science and Metallurgical Engineering, University of Pretoria, South Africa.

³Engineering Services, Armscor, Dockyard, Simon's Town, Cape Town, South Africa.

⁴Hulamin Operations Proprietary Limited, Moses Mabhida Road, South Africa.

Abstract. The effect of the extended soaking period in hours on the microstructure and mechanical properties of a modified AA3003mod clad with AA4045 for use in automobile heat exchangers investigated. The alloys were roll bonded to have a final thickness of 300 μm . Intermediate annealing (IA) was conducted during cold rolling at temperatures of between 270 and 350 $^{\circ}\text{C}$. The microstructures were investigated by using electron backscattered diffraction (EBSD). The fractographs of tensile-test specimens were analysed using the SEM-SEI. The UTS and YS of the samples soaked for longer residence times of 45 h, were found to be on the lower end of the 9031-H24 specification. Extended soaking time increased Al-Mn-Fe intermetallic phases observed on fracture surfaces, which degraded the yield strength ($R_{p0.2}$) by 35 MPa.

1 Introduction

Most automotive heat exchangers are typically fabricated by brazing 3xxx series aluminium alloy tubes clad with a silicon-containing 4xxx series alloy. During brazing at $\sim 600^{\circ}\text{C}$, the 4xxx cladding melts, forming joints. However, this process significantly reduces the strength of the 3xxx/4xxx materials, making them prone to deformation, sagging, or even leakage under operating conditions [1, 2]. Tubes are the most critical to the durability of the component, as tube failure (leakage) renders the entire heat exchanger inoperable. The properties of the post-brazed material are influenced by all production steps, which includes final cold rolling. Testing these properties is particularly challenging due to the thin gauge of tube materials (typically 0.2-0.5 mm) [3, 4].

The AA3003, as a typical representative of Al-Mn alloys, cannot be strengthened by heat treatments [3]. One of the most effective way to improve the properties of AA3003 is by alloying [5, 6]. According to the aforementioned research, it was demonstrated that the

* Corresponding author: josephm@mintek.co.za

addition of Cu encouraged solid solution strengthening. Moreover, Cu also aided in the formation of α -Al(Mn,Fe)Si dispersoids when brazing the AA3003-0.5Cu alloy while enhancing the dispersion strengthening mechanism. In this work the AA3003 was modified by addition of Cu. The effect of Cu on the microstructure and mechanical properties of the AA3003 before brazing was investigated. This work presented a comparative study of the microstructure and mechanical properties of the modified AA3003 clad with AA4045 for automobile heat exchangers. Since heat exchanger sheets are primarily supplied and used in the cold-rolled and annealed (CRA) state due to a combination of critical property requirements that this specific manufacturing process delivers. Therefore, this study focused instead on the impact of the soaking time on the CRA products mechanical properties.

2 Methodology and material

The materials used for this investigation were a modified AA3003 Al-Mn-Fe-Si alloy, AA4045/AA3003 mod supplied by Hulamin Rolled Products (Pty) Ltd. and processed as shown in Figure 1. The specific chemical compositions of each metal provided by the manufacturer are presented in Table 1. The composite sheet was manufactured out of AA4045 (clad layer) and AA3003mod (core layer). Firstly, AA3003 ingot was homogenized by soaking at 610 °C for 8 h (i.e. H24 practise), and the flat ingot of the clad layer was milled and hot-rolled to a thickness of 30 mm. Subsequently the two aluminium sheets (i.e. 3 mm AA4045 and 30 mm AA3003mod) were stacked, hot-roll bonded to between 8 and 10 mm thickness using upgraded Carl Wezel 2-high rolling mills (i.e. fitted with calibrated load-cells and the VT Scada Light rolling software to collect and process data), and then cold rolled to approximately 5 mm. Subsequently, samples were annealed at 330°C for 3 h and cold-rolled in multiple passes to a final thickness of 0.30 mm. Finally, the Al composite sheet with a thickness of 0.30 mm was obtained by tension levelling, trimming and final annealing to temper H24.



Fig 1: Methodology approach.

The two alloys that played a key role in this study was: (1) AA3003, which served as the reference / example alloy and, (2) a modified variant of AA3003 labelled as AA3003mod. AA3003 has the lowest mechanical strength among the alloys of the present investigation (i.e. YS of 50-125 MPa and UTS of 140 – 180 MPa). Chemical composition was determined by Inductively Coupled Plasma Optical Emission Spectroscopy (ICP-OES). To prepare cross-sections for microstructural analysis using electron backscattered diffraction (EBSD), the samples were electropolished with Struers A2 solution, a mixture of methanol and perchloric acid (80:20 ratio), at -10 °C and 35 V for 15 s after which it underwent diamond polishing on a Struers LectroPol-5 machine to a surface finish of 0.1µm. The EBSD data on the cold-rolled and annealed (CRA) samples was acquired on a Zeiss Cross Beam 540 Scanning Electron Microscope (SEM) equipped with Oxford Instrument’s NordLys EBSD cameras and Aztec Crystal EBSD software used to analyse the microstructures.

Tensile specimens from the cold rolled and annealed samples were extracted parallel to the rolling direction and tested at room temperature (RT) per ISO 6892-1:2019, using a 50 mm extensometer gauge length. Fracture morphology was examined via SEM imaging.

Based on the chemical composition of AA3003, the AA3003mod aluminium alloy was modified by adding a small amount of Cu and partially displacing Si and Fe in the crystal

structure. The cladding alloy, AA3003 and AA3003mod aluminium alloys' chemical compositions are given in Table 1.

Table 1: Chemical compositions of the alloys (wt.%).

Material	Elements (wt.%)						
	Si	Fe	Cu	Mn	Mg	Cr	Al
AA3003	0.60	0.70	0.05 – 0.20	1.0 – 1.5	-	-	Bal
AA3003 mod	0.06	0.20	0.42	1.50	0.21	0.01	Bal
AA4045	10.1	0.15	-	0.02	0.01	-	Bal

3 Results and discussion

3.1 Microstructures and mechanical properties

The electron backscatter diffraction (EBSD) was used to quantify the grain size evolution post-annealing. Figure 2. Presented the EBSD orientation maps of AA3003mod after it had been reheated at 505 °C by means of varying holding times, to achieve a CRA structure. These microstructural differences further revealed distinct colour variations in the EBSD patterns (Figures 2a and b), indicating more crystallographic orientation changes. Furthermore, a mixture of fine and coarse grains was observed which were not impacted by a variation in the homogenization time.

Table 2 summarises the tensile testing results, which include yield strength ($R_{p0.2}$) determined by an averaged taken from three tests per condition, along with comparative data and AA3003mod (AA9031) tubestock specifications (minimum elongation: 8%). The tested $R_{p0.2}$ and R_m values in Table 2 align with A3003 alloy specifications (e.g., 20 h-CRA: ~150 MPa yield, 270 MPa ultimate strength). As may be seen, the YS of specimens soaked for 45 h was below specification because excessive time at 505°C caused excessive grain growth and annihilation of dislocations, overcoming the strengthening effect of the dispersoids. The 20 h annealed sample displays grains ranging from 6.15 to 116.82 μm , while the 45 h sample had more of the larger grains ranging from 6.15 to 194.75 μm . EBSD is not just a qualitative imaging technique; it is a premier quantitative tool for microstructural statistics. The ability to measure the median grain size from a full distribution of thousands of grains provides an objective, precise, and statistically significant metric to quantify the effect of altered processing conditions on microstructure.

As part of a standard operating procedure, the clad ingots are usually held in the reheating furnace and soaked for a period of below 30 h before rolling. However, if there is an equipment breakdown during processing, this will result in the ingots being left in the furnace at the set temperature for longer periods. This study found that CRA specimens soaked at 45 h during processing failed to meet target specifications due to prolonged exposure at 505°C in the preheat furnace.

Microstructural analysis of these samples revealed coarse Mn dispersoids formed during preheating, and a contraction as an indication of lack of recrystallisation (RX) [7, 8]. Coarse dispersoids promote premature recrystallization during temper annealing, weakening the material (reduced yield/tensile strength) (Table 2).

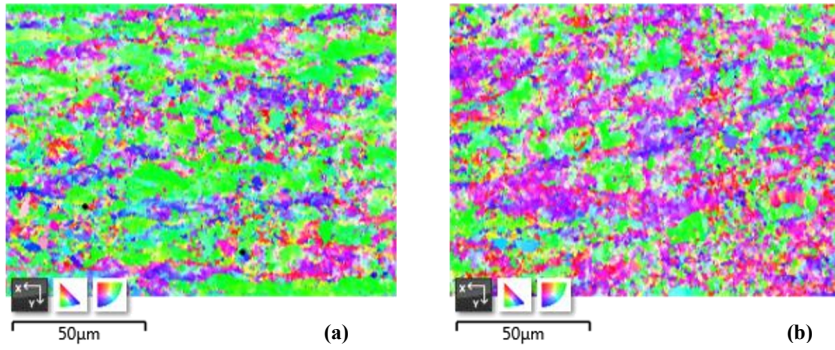


Fig 2: EBSD IPF micrograph of AA4045/AA3003mod Al clad sheet in various conditions - (a) cold-rolled and (b) 330°C/3 h annealed and unbrazed (partially recovered material).

The AA3003 core band contrast maps, show evidence of partial recrystallised grains, likely due to insufficient recovery, where high dislocation density from prior rolling reduced indexing rates (Figure 3). The Mn addition promotes precipitate formation in the core, hindering grain boundary migration, elevating recrystallization temperatures, and impeding recovery and/or recrystallization (Figure 3b).

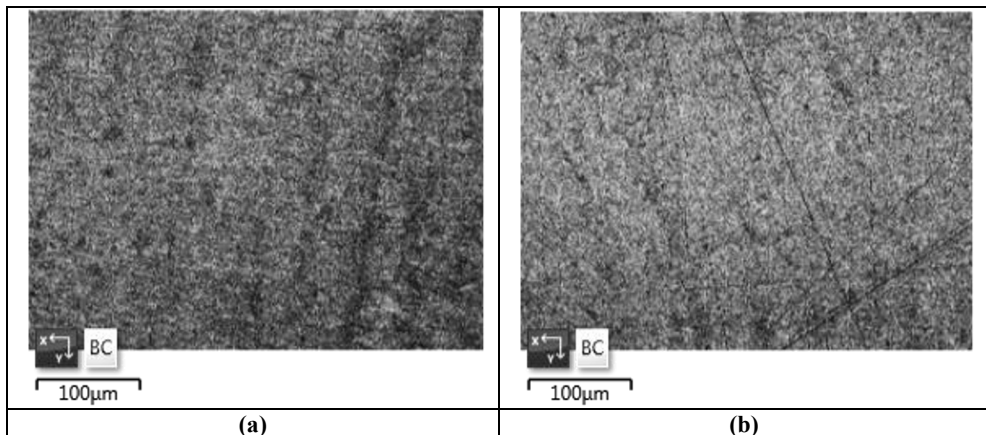


Fig 3: EBSD band contrast (BC) maps of AA4045/AA3003mod Al clad sheet in - (a) cold-rolled condition and (b), 330°C/3 h annealed and unbrazed.

Table 2: Mechanical properties of roll bonded AA4045/AA3003mod aluminium brazing sheets.

Material	Mechanical properties (MPa)		
	YS ($R_{p0.2}$)	UTS (R_m)	Elongation (%)
AA3003 commercial [3]	50-125	140 - 180	25-36
AA3003mod specification	145 (minimum)	190 - 230	8
AA3003 20 hr	150	270	7.8
AA3003 45 hr	111	217	9.8

Figure 4 shows the fracture morphology of the modified AA3003-AA4045 clad sheet soaked for 20 and 45 h. A typical ductile fracture with a mixture of large, deep and small dimples and the bonding interfaces that remained intact are visible in Figure 4a. Specimen that were processed for 20 h exhibited larger, deeper dimples, which correlated well with higher yield ($R_{p0.2}$) and tensile (R_m) strengths (Table 2), while in the 45 h sample smaller, shallower dimples consistent with declining mechanical performance were visible (Figure

4b). Although micropores and secondary particles are dispersed across fractures, equiaxed dimples confirm ductile fracture failure [9].

Two dimple types were observed, namely: sparsely distributed large dimples and densely distributed small dimples (Figure 4b). Energy-dispersive X-ray (EDX) spectroscopy was used to identify coarse particles (arrows in Figure 4a), rich in Mn, Fe, Al, and Si (Mn > Fe) that were harmful to the mechanical properties of the metal could promote crack nucleation and alter dimple morphology [8]. These second-phase particles, along with inclusions on grain boundaries, act as strain discontinuities that initiate microvoids (Figures 5a and 6a). Decohesion of particles from the matrix creates the dimpled appearance, with voids coalescing during failure [8, 9]. Figure 5a further illustrates fractures in Fe-Cu intermetallics, underscoring their role in weakening the alloy. Extended soaking time increased Al-Mn-Fe intermetallic phases (observed on fracture surfaces in Figure 6a), which would degrade the mechanical performance.

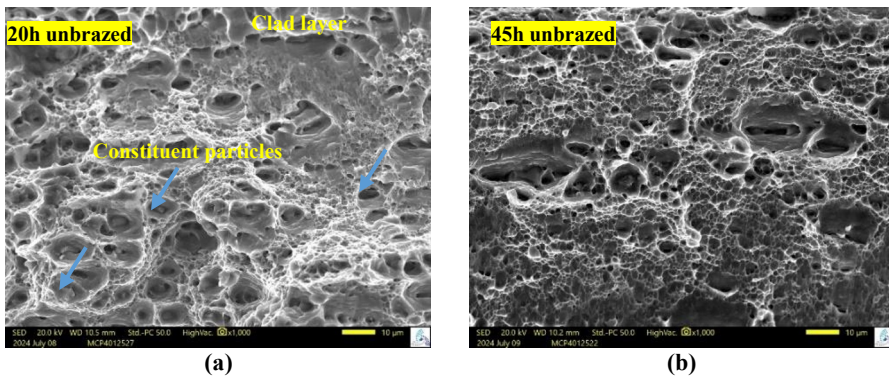
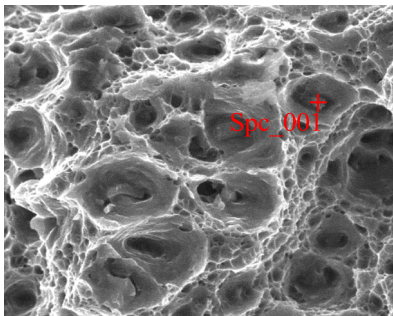


Fig 4: Fractographs of AA4045/AA3003mod Al clad sheet in various conditions - (a) cold-rolled, 330°C/3 h annealed and, (b) unbrazed.



Elements	Mass%	Atom%
Al	88.69±0.40	94.14±0.42
Mn	6.77±0.20	3.53±0.11
Fe	4.54±0.18	2.33±0.09
Total	100.00	100.00

10 µm

(a) 20 h

(b)

Fig 5: Fractography of AA4045/AA3003mod Al clad sheet showing - (a) SEM-EDS spot analyses on the constituent particles and, (b) the compositions in (wt% and at.%) of these constituent particles identified as aluminium ; iron, and manganese.

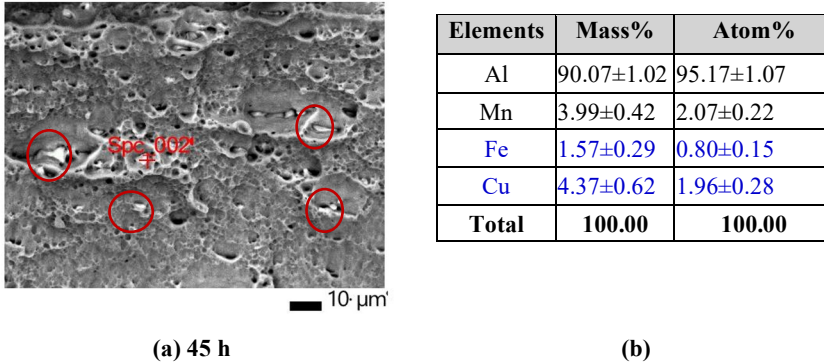


Fig 6. Fractography of AA4045/AA3003mod Al clad sheet showing - (a) SEM-EDS spot analyses on the constituent particles and, (b) the compositions in of the constituent particles. Undissolved Cu containing phase marked with red circles.

4 Conclusion

The effects of soaking time on the mechanical properties of AA3003mod clad with AA4045 alloy (9031-H24 tube stock) were investigated and the following conclusion drawn:

- The sample soaked for 45 h exhibited 40% larger grain size even after cold rolling and annealing, which suggested an undesirable effect in industrial processing because it prevents the formation of a random, homogeneous microstructure.
- The YS, $R_{p0.2}$, and UTS, R_m , of the sample soaked for 20 h were found to be within the specifications of the AA3003 i.e., YS of 145 MPa and UTS of 190-230 MPa. Conversely, the sample soaked for 45 h did not meet the YS specification and this was attributed to the coarsening of its microstructures.
- Both samples demonstrated ductile fractures with a mixture of large, deep and small dimples. However, the 20 h sample showed more of the deep dimples.
- Si particles acted as crack initiation sites and intermittently through Fe-rich intermetallic phases weakening the mechanical properties of the sample.

The authors would like to thank Mintek South Africa for financial support and Hualamin Rolled Products (Pty) Ltd for supplying materials, as well as Mbavhalelo Maumela and Richard Mathebula for their involvement during the roll-bonding process.

The Department of Science Technology and Innovation (DSTI) - Advanced Materials Initiative (AMI), through the Ferrous Materials Development Network (FMDN), financially supported this work, in addition to the Department of Minerals, Petroleum and Energy (DMPE) through Mintek Science Vote programme.

References

- [1] Z. Yuan, Y. Tu, T. Yuan, Y. Huang, Y. Zhang, Gradient multilayer aluminium sheets used in automotive heat exchangers. *J. Mater. Sci.* **56(8)**, 5215 (2021).
<https://doi.org/10.1007/s10853-020-05584-5>
- [2] C. Liu, X. Xue, X. Chen, L. Li, C. Xia, Z. Zhong, D. Zhou, Effect of microstructural evolution on sagging behaviour of cold-rolled aluminium foil during the brazing thermal cycle. *J. of Materi. Eng. and Perform.* **26**, 5563 (2017).
<https://doi.org/10.1007/s11665-017-2782-8>

- [3] S. Kahl, H.E Ekström and J. Mendoza, Tensile, fatigue, and creep properties of aluminium heat exchanger tube alloys for temperatures from 293 K to 573 K (20 °C to 300 °C). *Metall Mater Trans A* **45**, 663 (2014).
<https://doi.org/10.1007/s11661-013-2003-5>
- [4] W. Zheng, C. Ni, C. Xia, S. Deng, X. Jiang and W. Xu, High-temperature mechanical properties and microstructure of ultrathin 3003mod aluminium alloy fins. *Metals*, **14**, 142 (2024). <https://doi.org/10.3390/met14020142>
- [5] Z. Li, Z. Zhang and X.G. Chen, Microstructure, elevated-temperature mechanical properties and creep resistance of dispersoid-strengthened Al-Mn-Mg 3xxx alloys with varying Mg and Si contents. *Mater. Sci. Eng. A*. **708**, 383 (2017).
<https://doi.org/10.1016/j.msea.2017.10.013>
- [6] Z. Li and X.G. Chen, Effect of magnesium on dispersoid strengthening of Al—Mn—Mg—Si (3xxx) alloys. *Trans. Nonferrous Met. Soc. China*. **26**, (11), 2793 (2016).
[https://doi.org/10.1016/S1003-6326\(16\)64407-2](https://doi.org/10.1016/S1003-6326(16)64407-2)
- [7] J.S. Moema, C.W Siyasiya; V.K. Morudu and T. Buthelezi, The Effect of Soaking Time on Mechanical Properties of Roll-Bonded AA3003 and AA4045 Used for Heat Exchangers. *Metals*, **13**, 1636 (2023). <https://doi.org/10.3390/met13101636>
- [8] J.S. Moema, C.W. Siyasiya, K.V. Morudu, N.D. Hadebe, T. Buthelezi, An investigation on SWAAT and electrochemical corrosion behaviour of roll-bonded and brazed aluminium alloy - AA4045/AA3003, MATEC Web Conf., **388**, 03002, (2023).
<https://doi.org/10.1051/mateconf/202338803002>
- [9] P. Maruschak, I. Konovalenko, A. Sorochnikov, Methods for evaluating fracture patterns of polycrystalline materials based on the parameter analysis of ductile separation dimples: A review. *Engineering Failure Analysis*, **153**, 107587 (2023).
<https://doi.org/10.1016/j.engfailanal.2023.107587>